Nanotechnology **19** (2008) 495706 (7pp) doi:10.1088/0957-4484/19/49/495706

Enhanced ionic conductivity of AgI nanowires/AAO composites fabricated by a simple approach

Li-Feng Liu[1], Seung-Woo Lee[2,3], Jing-Bo Li[4], Marin Alexe[1], Guang-Hui Rao[4], Wei-Ya Zhou[4], Jae-Jong Lee[3], Woo Lee[1,5] and Ulrich Gösele[1]

[1] Max Planck Institute of Microstructure Physics, Weinberg 2, D-06120 Halle, Germany
[2] University of Science and Technology (UST), Yuseong, 305-333 Daejon, Korea
[3] Korea Institute of Machinery and Materials (KIMM), Yuseong, 305-343 Daejon, Korea
[4] Beijing National Laboratory for Condensed Matter Physics and Institute of Physics, Chinese Academy of Sciences, Beijing 100190, People's Republic of China
[5] Korea Research Institute of Standards and Science (KRISS), Yuseong, 305-340 Daejon, Korea

E-mail: woolee@kriss.re.kr

Received 14 August 2008, in final form 16 October 2008
Published 19 November 2008
Online at stacks.iop.org/Nano/19/495706

Abstract

AgI nanowires/anodic aluminum oxide (AgI NWs/AAO) composites have been fabricated by a simple approach, which involves the thermal melting of AgI powders on the surface of the AAO membrane, followed by the infiltration of the molten AgI inside the nanochannels. As-prepared AgI nanowires have corrugated outer surfaces and are polycrystalline according to scanning electron microscopy (SEM) and transmission electron microscopy (TEM) observations. X-ray diffraction (XRD) shows that a considerable amount of 7H polytype AgI exists in the composites, which is supposed to arise from the interfacial interactions between the embedded AgI and the alumina. AC conductivity measurements for the AgI nanowires/AAO composites exhibit a notable conductivity enhancement by three orders of magnitude at room temperature compared with that of pristine bulk AgI. Furthermore, a large conductivity hysteresis and abnormal conductivity transitions were observed in the temperature-dependent conductivity measurements, from which an ionic conductivity as high as $8.0 \times 10^2\ \Omega^{-1}\ \mathrm{cm}^{-1}$ was obtained at around 70 °C upon cooling. The differential scanning calorimetry (DSC) result demonstrates a similar phase transition behavior as that found in the AC conductivity measurements. The enhanced ionic conductivity, as well as the abnormal phase transitions, can be explained in terms of the existence of the highly conducting 7H polytype AgI and the formation of well-defined conduction paths in the composites.

S Supplementary data are available from stacks.iop.org/Nano/19/495706

(Some figures in this article are in colour only in the electronic version)

1. Introduction

Silver iodide (AgI) is a superionic conductor which has extensively been studied for many decades due to its high ionic conductivity compared to other monovalent cation conductors [1]. It is well documented that, when AgI is homogeneously mixed with a solid insulating compound (e.g. γ-Al_2O_3, SiO_2, etc), the conductivity of the resulting composite will be greatly enhanced. For this reason, AgI-based composite solid electrolytes have attracted considerable research interest [1–7]. Although the microscopic mechanism responsible for the marked conductivity enhancement is not well understood, it is generally accepted that the space charge regions between AgI and the insulating oxide

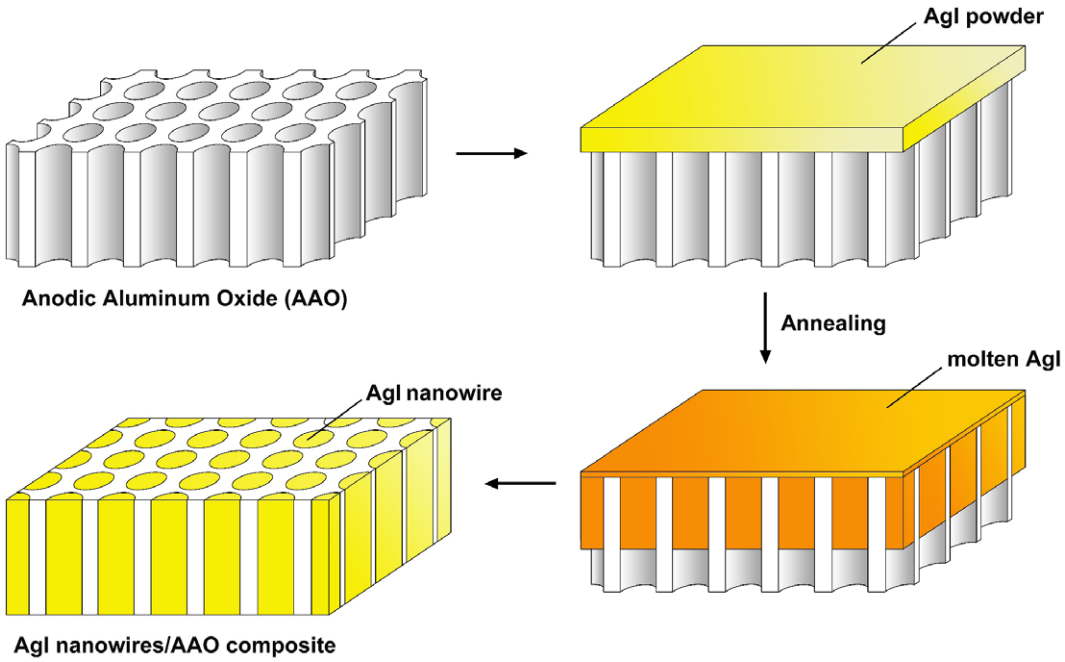

Figure 1. Schematic illustration of the fabrication of AgI NWs/AAO composites.

matrix play an important role [4]. In addition, it is also believed that the formation of an interfacial conducting phase (AgI with 7H stacking fault arrangements, ABCBCAC) has a significant contribution to the enhancement of ionic conductivity in the AgI/oxide composites [8]. Recently, composite electrolytes consisting of AgI nanowires (NWs) and porous anodic aluminum oxide (AAO) (i.e. AgI NWs/AAO composites) were realized by different methods, such as gaseous iodination [9], paired-cell reaction [10–12] and step-electrochemical iodination [13, 14]. Aside from its excellent thermal and mechanical stabilities, the well-organized nanoporous structure of the AAO membrane could provide well-defined ion conduction paths for the AgI NWs/AAO composites [9, 13], which may potentially facilitate the enhancement of ionic conductivity. Therefore, AgI NWs/AAO composites are thought to be applicable in electrochemical devices such as batteries and sensors [14].

Here, we report on a novel and simple approach to the fabrication of AgI NWs/AAO composites, which involves the thermal melting of AgI powders on the surface of AAO membranes, followed by the infiltration of the molten AgI into the nanochannels of the AAO. This approach not only allows a rapid synthesis of well-defined AgI NWs/AAO composites, but also can enhance the room temperature ion conductivity by two to three orders of magnitude, compared to the pristine bulk AgI. The morphology, structure and phase transitions of the as-prepared AgI NWs/AAO composites were investigated in detail. The possible mechanisms responsible for the conductivity enhancement are discussed.

2. Experimental section

The AAO membranes used here were prepared by a two-step anodization process in phosphoric acid solution, as described previously [15]. After the second anodization, the underlying aluminum substrate was etched away by a mixture of $CuCl_2$ and HCl. Subsequently, the barrier layer was removed by a 10 wt% H_3PO_4 solution at 45 °C for 50 min to obtain through-hole membranes. The average pore diameter and the thickness of as-prepared AAO membranes are 220 nm and 90 μm, respectively.

AgI NWs/AAO composites were prepared by melt impregnation of solid AgI into AAO membranes as schematically illustrated in figure 1. First, a piece of through-hole AAO membrane was directly placed onto a fast heating/cooling furnace (Eurotherm temperature controller 808). An excess amount of AgI powder (Sigma-Aldrich, 99.9%) was loaded on the surface of the AAO membrane in order to ensure complete filling of the oxide nanopores, heated rapidly to 650 °C at a rate of 210 °C min^{-1}, well above the melting point of the pristine AgI (m.p. = 558 °C) [16], and then annealed at this temperature for 20–30 min. Afterward, the sample was cooled down to 200 °C at a rate of 100 °C min^{-1} and then gradually to room temperature within 30 min. During the whole heating cycle, the sample was kept in the dark by covering it with aluminum foil to avoid photodecomposition of the AgI. It was observed that AgI powder starts to melt at around 560 °C to wet the entire surface of the membrane, and to infiltrate into the oxide nanopores driven by gravity and the surface interaction between the molten AgI and the oxide surface. For an AAO membrane with a thickness of 90 μm, it only took about 20 min to achieve complete filling of the nanochannels, which turned out to be much faster than other preparation methods reported previously [13, 14].

The morphology of as-prepared AgI NWs/AAO composites was examined by scanning electron microscopy (SEM, JEOL JSM-6340F) and transmission electron microscopy

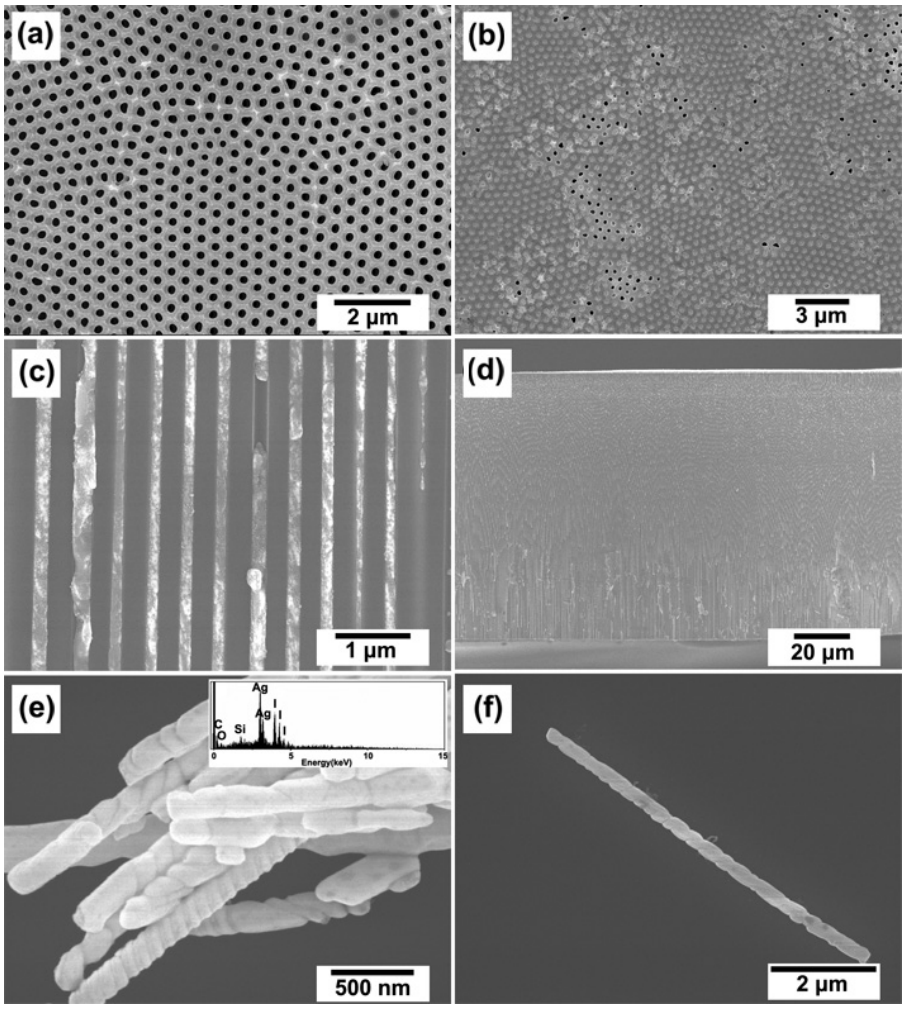

Figure 2. SEM micrographs of (a) an empty AAO membrane; (b) plan view and ((c), (d)) cross-sectional view of the AgI NWs/AAO composite; ((e), (f)) AgI NWs released from the AAO matrix. Inset of (e): EDX spectrum.

(TEM, JEOL JEM-1010). Specimens for microscopic investigations were prepared by completely dissolving the AAO templates with 1 M NaOH solution at 45 °C for several hours, and the resulting nanowire suspension was centrifuged to collect the nanowires. AgI NWs were rinsed in deionized water several times and finally washed in ethanol. They were then deposited on a piece of silicon substrate and a carbon-coated Cu grid for SEM and TEM investigations, respectively. Phases of the sample were analyzed using an x-ray diffractometer (XRD, Philips X'Pert MRD) equipped with Cu Kα radiation ($\lambda = 1.5406$ Å). The scanning rate was set as $0.0008°\ s^{-1}$. Thermal analyses were carried out with a differential scanning calorimeter (DSC, TA-Q200) over a temperature range from 0 to 250 °C. Both heating and cooling rates are $2\,°C\ min^{-1}$. The temperature-dependent ionic conductivity was measured with an impedance analyzer (Hewlett-Packard HP 4192A, see figure 5(a) for measurement configuration). For conductivity measurements, both surfaces of the AgI NWs/AAO composite were partially etched with 1 M NaOH at 45 °C for 30 s, through which the AgI thin film covering on the surfaces of the AAO membrane could easily be detached. Subsequently, a thin layer of Ag (approx. 200 nm) was sputtered on one side of the sample, while an array of Ag microelectrodes was constructed on the other side by sputtering Ag through a shadow mask.

3. Results and discussions

Figure 2 shows typical SEM micrographs of an empty AAO membrane (figure 2(a)), plan (figure 2(b)) and cross-sectional views (figures 2(c) and (d)) of the AgI NWs/AAO composite, and AgI NWs liberated from the AAO matrix (figures 2(e) and (f)). According to image analysis based on figure 2(a), the average pore diameter and interpore distance of the AAO membrane turned out to be 220 nm and 460 nm, respectively. Melt impregnation of AgI resulted in filling of the oxide nanopores, and the filling density was estimated to be around 80%. Parallel alignment of AgI NWs in the alumina matrix is evident from the cross-sectional SEM micrograph, as shown in figure 2(c). Complete filling of AgI throughout the entire length of the nanopores was confirmed by cross-sectional SEM (figure 2(d)). Figures 2(e) and (f) show representative SEM images of AgI NWs freed from the alumina matrix by removing the AAO membrane with 1 M NaOH solution. It was found that the morphology of most

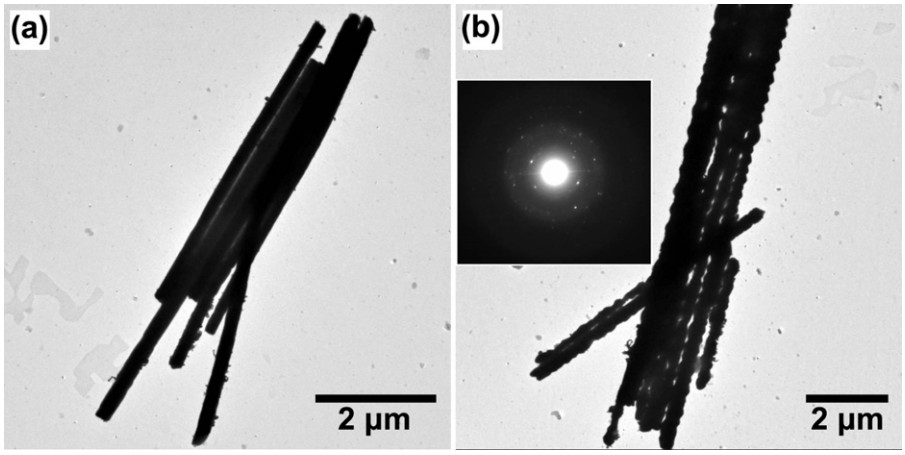

Figure 3. TEM micrographs of as-prepared AgI NWs. (a) AgI NWs with smooth outer surfaces; (b) AgI NWs with corrugated surfaces. Inset: electron diffraction pattern.

AgI NWs is characterized by a corrugated outer surface. A smaller percentage shows a smooth surface. AgI NWs with a corrugated outer surface appear to be twisted, forming a spiral topography. The evolution of the corrugated outer surfaces is not clear. We speculate that the viscous flow and the relatively fast cooling rate of molten AgI inside the oxide nanopores have a certain relevance to this topographical evolution. The energy-dispersive x-ray (EDX) spectrum shown in the inset of figure 2(e) confirms that the as-obtained nanowires consist of silver and iodine. The Si, C and O peaks originate from the silicon wafer and the conductive carbon tape which were used for the SEM observation.

Figures 3(a) and (b) show the TEM images of as-prepared AgI NWs with smooth and corrugated outer surfaces, respectively. It was found that the AgI NWs are unstable during the TEM investigation. Upon irradiation by the electron beam, the NWs were subject to a quick decomposition, especially at a high magnification, which made it difficult to analyze their microstructure in detail. Shown in the inset of figure 3(b) is a quick-snap electron-diffraction (ED) pattern of as-prepared AgI NWs, which demonstrates that the NWs are crystalline.

In order to identify the phases of the AgI NWs/AAO composites, XRD measurements were performed over a wide 2θ range. Figures 4(a) and (b) show XRD patterns of as-prepared AgI NWs/AAO composites and commercially available pristine AgI powder as a comparison, respectively. According to figure 4(b), the commercial AgI powders are composed of a mixture of β-AgI and γ-AgI. No diffraction peaks from other phases or impurities were detected. In contrast, the XRD pattern of AgI NWs/AAO composites exhibits different features. It is evident from figure 4(a) that some peaks of $\beta(h0l)$ diffractions have significantly weakened or even disappeared, as denoted by blue dashed lines; meanwhile, new diffraction peaks neighboring $\beta(101)$, $\beta(102)$, $\beta(103)$ and $\beta(203)$ on both sides appear in the XRD pattern (red dotted lines). This observation is in good accordance with earlier studies on AgI/Al_2O_3 composites [8, 17] and suggests that a new phase, which has been termed 7H polytype AgI (stacking fault ABCBCAC), emerges in the AgI NWs/AAO composite. Although the

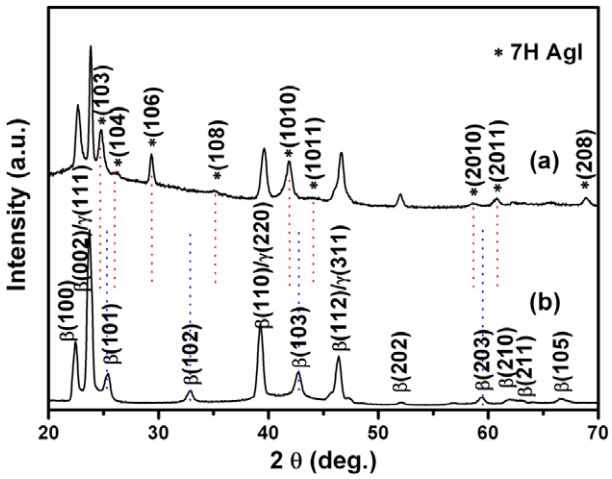

Figure 4. XRD pattern of (a) AgI NWs/AAO composite and (b) commercial AgI powders.

existence of 7H polytype AgI has long been postulated as one of the major contributions to the marked enhancement in ionic conductivity of AgI/Al_2O_3 composite electrolytes, the presence of 7H-AgI was experimentally demonstrated only very recently [8]. In figure 4(a), it is found that the diffraction peaks which come from 7H polytype AgI and are indexed by stars can be clearly distinguished. What is more, these 7H-AgI diffraction peaks are even more pronounced than those in the earlier reports [8, 17, 18], unambiguously demonstrating the existence of a considerable amount of 7H polytype in our AgI NWs/AAO composite.

It is believed that the formation of 7H-AgI stacking faults in the composites is due to the strong chemical interaction between AgI and alumina. It is well known that the inner walls of an AAO membrane are usually terminated with hydroxide groups [19]. The surface hydroxide groups can absorb silver ions from the embedded AgI NWs, and thus create lattice disorder in AgI, offering a driving force high enough to trigger the formation of the 7H polytype [8]. It was also pointed out that annealing at a high temperature (>558 °C, m.p. of

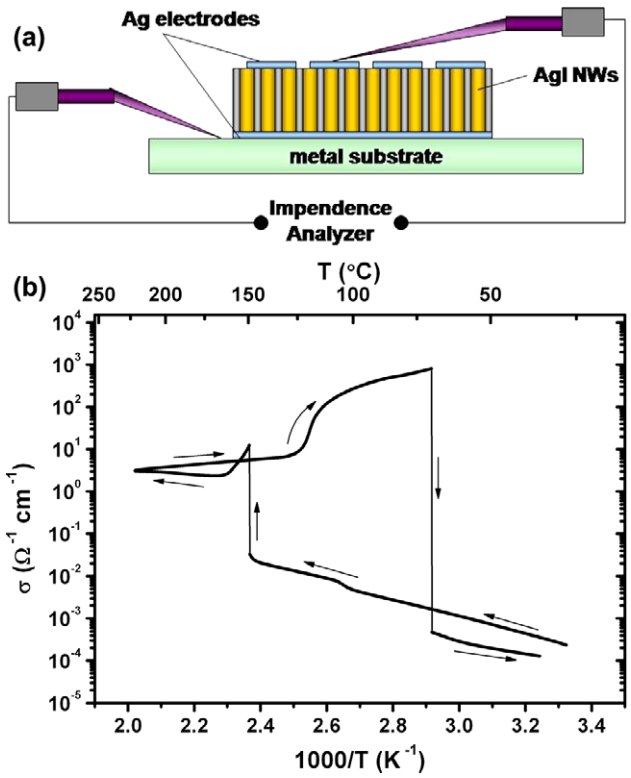

Figure 5. (a) Schematic illustration of the ionic conductivity measurement of as-prepared AgI NWs/AAO composite; (b) temperature-dependent ionic conductivity of as-prepared AgI NWs/AAO composite.

AgI) facilitates the formation of polytype AgI because it improves interfacial contact between AgI and alumina, and thus promotes propagation of the phase transformation through the agglomerated AgI crystallites [8]. In the present study, the AgI NWs/AAO composites were obtained by infiltrating the molten AgI into the nanochannels of the AAO membrane at a high temperature (650 °C). In this process, the molten AgI should have a good contact with the inner surface of the nanochannels. In addition, the turbulence of the AgI melts inside the nanopores may induce a large amount of grain boundaries, defects or stacking faults, which is reflected by the corrugated surface morphology of the dispersed AgI NWs (figures 2(e) and (f)). We assume that all these factors contributed to the formation of 7H-AgI. According to the previous study [8, 20], excess iodine and the high surface area are important for stabilizing the 7H-AgI. The excess AgI powder used in our experiments and the high surface area of the AAO membrane meet these conditions well, and therefore are expected to make a major contribution to the observation of 7H-AgI in the as-prepared AgI NWs/AAO composite at room temperature.

The ionic conductivity of the as-prepared AgI NWs/AAO composites was measured by applying an ac potential on both sides of the composites. Figure 5(a) shows the schematic diagram for the measurement configuration. The area of the top silver microelectrodes is approximately 0.09 cm^2. The ionic conductivity was found to be frequency-dependent (see supporting information available at stacks.iop.org/Nano/19/495706). A representative temperature-dependent conductivity curve, which was measured at 1 kHz, is plotted in figure 5(b). The effective conductivity was calculated by taking the following parameters into account: the filling density of AgI NWs (∼80%), the pore density (5.46×10^8 cm^{-2}), the diameter (220 nm) and the length (90 μm) of the nanopores. Ionic conductivity at room temperature was found to be 2.3×10^{-4} Ω^{-1} cm^{-1}, which is almost three orders of magnitude higher than that of pristine AgI (3×10^{-7} Ω^{-1} cm^{-1}) [2].

According to figure 5(b), the conductivity first increases slowly with increasing temperature and then shows a small upwards jump at around 100 °C. At 149 °C, the conductivity exhibits a sharp increase (reaching 12.4 Ω^{-1} cm^{-1}), manifesting a phase transition from β/γ-AgI to superionically conductive α-AgI. The transition temperature is slightly higher than that of the pristine bulk AgI (147 °C). Subsequently, the conductivity quickly decreases to 2.3 Ω^{-1} cm^{-1} and then increases slowly again with further increase in temperature. Upon cooling, the conductivity first increases as the temperature decreases. Starting from 120 °C, the conductivity increased rapidly and reached 8.0×10^2 Ω^{-1} cm^{-1} at 70 °C. To the best of our knowledge, this is the highest ionic conductivity observed in AgI-based systems. Then, a dramatic conductivity decrease occurs with further decrease in temperature, which corresponds to the phase transition from α-AgI to β/γ-AgI.

Compared with the previous studies, the temperature-dependent conductivity curve presented here has three different characteristics as follows. First, in addition to the main conductivity transitions coming from $\beta/\gamma \leftrightarrow \alpha$ phase transitions, there are other transitions (100 °C on heating and 120 °C on cooling) in our samples, which have not yet been reported previously. Second, an abnormal conductivity increase upon cooling was observed for the first time. In general, the conductivity decreases or remains unchanged upon cooling over a certain temperature range below the α-AgI $\rightarrow$ β/γ-AgI phase transition at 147 °C, irrespective of the composition of samples (i.e. pristine AgI or AgI/Al_2O_3 composites). In the present study, however, the ionic conductivity of the samples increased by two orders of magnitude in the temperature range of 130–110 °C upon cooling. It is assumed that this abnormal conductivity enhancement could be related to the formation of well-defined conduction paths between the embedded AgI NWs and the inner walls of the alumina. As discussed above, the 7H-AgI preferentially forms at the interfaces between AgI NWs and the inner walls of the AAO membrane. AgI has a negative thermal expansion coefficient (approx. -2×10^{-6} K^{-1} at 100 °C) [14, 21] and thus undergoes a volume expansion upon cooling. In this case, it is possible that much more highly conducting 7H-AgI is formed at the interfaces. Because of the straight and unidirectional nature of the pore walls of the AAO membrane (i.e. the interfaces between AgI NWs and the alumina), the highly conducting 7H phases may connect with each other and form continuous conduction paths, thus leading to the enhancement of ionic conductivity. Third, the temperature-dependent conductivity curve exhibits a wide hysteresis and a very sharp conductivity transition at 70 °C

(α-AgI $\rightarrow$ β/γ-AgI). The hysteresis of ionic conductivity in AgI/oxide composites upon heating and cooling has been observed and studied extensively [2, 6, 8, 14, 17]. It mainly arises from the phase transitions from β/γ-AgI to superionconducting α-AgI upon heating and from α-AgI to β/γ-AgI upon cooling. The magnitude of hysteresis was found to depend on the molar ratio of the AgI to the alumina [2, 3, 6, 8, 17]. More recently, very broad conductivity hysteresis and gradual conductivity decrease upon cooling were also found in AgI NWs/AAO composites, and were ascribed to the retarded phase transition from α-AgI to β/γ-AgI [14]. In the present study, it is believed that two competing processes co-exist over the temperature range of 130–70 °C. One process is the formation of the well-defined conduction paths and the other is the gradual phase transition from α-AgI to β/γ-AgI, which would result in the slow decrease in conductivity. Obviously, the former process dominates in this temperature range, thus leading to the abnormal increase of the conductivity. In the meantime, the transition from highly conducting α-AgI to β/γ-AgI occurs simultaneously upon cooling. At around 70 °C, almost all α-AgI is transformed into β/γ-AgI, giving rise to the sharp drop in conductivity. It is expected that, thanks to the sharp and marked conductivity transitions, the composites may have a potential application in temperature sensors.

To analyze the phase transition processes in more detail, differential scanning calorimetry (DSC) was carried out. Figure 6 displays DSC curves observed for the AgI NWs/AAO composite. The phase transition of the sample can correlate very well with the temperature-dependent ionic conductivity shown in figure 5(b). Two distinct endothermic peaks at 100 and 149 °C were observed upon heating of the sample. The peak at 149 °C can be ascribed to the structural transformation from β/γ-AgI to α-AgI, in conjunction with the result of conductivity measurements, while the peak at around 100 °C can be assigned to the phase transition from metastable zinc blende γ-AgI to wurtzite β-AgI that is usually stable below the normal phase transition temperature (147 °C). Previously, it was reported that the phase transformation from γ-AgI to β-AgI occurred in the range 120–130 °C, and varied with the composition ratio of γ-AgI to β-AgI in the precursors [22]. In our case, the observed transition temperature is about 20 °C lower. Although the reason for the lower transition temperature is not completely understood, it might be associated with the size effect of the AgI NWs. It is also noted that, compared with the AgI NWs/AAO composite produced by the iodination of electrodeposited Ag NWs [14], no superheating behavior was observed in our sample. The phase transition from β/γ-AgI to α-AgI occurs at 149 °C, which is exactly the same as the conductivity transition temperature, but slightly higher than that of the bulk pristine AgI (147 °C).

Upon cooling, there are no exothermic peaks at 149 and 100 °C. Instead, three weak and broad exothermic peaks were detected at 120, 70 and 45 °C, as clearly shown in the inset of figure 6. The thermal event occurring at around 120 °C should be closely correlated with the abnormal conductivity increase, as is depicted in figure 5(b), which possibly corresponds to the α $\rightarrow$ 7H phase transition, while the broad exothermal

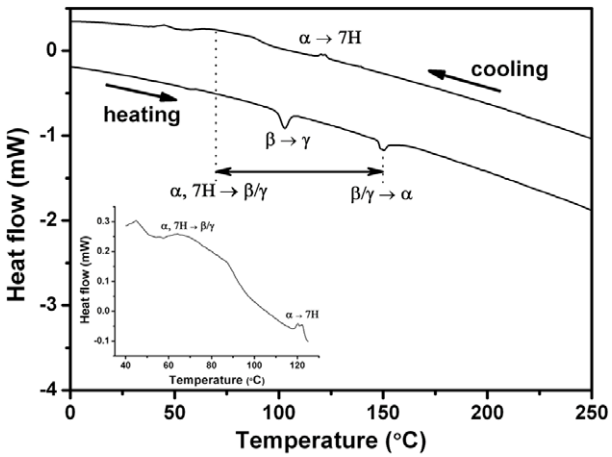

Figure 6. DSC heating and cooling curves of AgI NWs/AAO composite. Inset: the magnified profile in the cooling stage.

peak centered at 70 °C can be assigned to the phase transition from α-AgI to β/γ-AgI, taking the conductivity measurement results into account. It is believed that the broadened shoulder appearing in the range of 100–70 °C stems from the gradual phase transition of α $\rightarrow$ β/γ, as mentioned above. The exothermal peak at 45 °C, unfortunately, cannot find a corresponding transition in figure 5(b) and its origin is not clear at the moment. To further clarify the phase transition behaviors and identify the structural evolution of the as-prepared AgI NWs/AAO composites, *in situ* XRD investigations are needed and will be carried out in a future study.

4. Conclusions

In summary, we describe a simple method for the fabrication of AgI nanowires/AAO composites. By thermal melting of AgI powders on the surface of a through-hole AAO membrane and the subsequent infiltration of the molten AgI into the oxide nanopores, AgI NWs/AAO composites can be readily obtained. It was found that most of the as-prepared AgI nanowires had corrugated outer surfaces and were polycrystalline. A considerable amount of highly conducting 7H polytype AgI was found in the composites, which should be responsible for the enhancement of ionic conductivity at room temperature. Temperature-dependent conductivity of the as-prepared AgI NWs/AAO composites were measured, and an ionic conductivity as high as $8 \times 10^2\ \Omega^{-1}\ \mathrm{cm}^{-1}$ was observed and could be explained in terms of the formation of well-defined unidirectional conduction paths along the pore walls of the alumina membrane. The temperature-dependent phase transition was investigated by differential scanning calorimetry. The results showed a good correlation with the temperature-dependent conductivity measurements. It is expected that the present AgI NWs/AAO composites could find uses in many applications such as solid-state batteries or temperature sensors. Moreover, the synthetic approach reported here can be easily extended to the fabrication of other low-melting-point compound nanowires.

Acknowledgment

SWL is grateful for the financial support of the Korea Research Foundation Grant funded by the Korean Government (MOEHRD) (KRF-2007-612-D00103) during his stay at MPI-Halle.

References

[1] Agrawal R C and Gupta R K 1999 *J. Mater. Sci.* **34** 1131
[2] Shahi K and Wagner J B 1981 *J. Electrochem. Soc.* **128** 6
[3] Nagai M and Nishino T 1991 *J. Electrochem. Soc.* **138** L49
[4] Maier J 1995 *Prog. Solid State Chem.* **23** 171
[5] Uvarov N F, Vanek P, Savinov M, Zelezny V, Studnicka V and Petzelt J 2000 *Solid State Ion.* **127** 253
[6] Yamada H, Bhattacharyya A J and Maier J 2006 *Adv. Funct. Mater.* **16** 525
[7] Albert S, Frolet N, Yot P, Pradel A and Ribes M 2006 *Solid State Ion.* **177** 3009
[8] Lee J S, Adams S and Maier J 2000 *J. Electrochem. Soc.* **147** 2407
[9] Lee W, Yoo H I and Lee J K 2001 *Chem. Commun.* 2530
[10] Piao Y Z and Kim H 2003 *Chem. Commun.* 2898
[11] Wang Y H, Ye C H, Wang G Z, Zhang L D, Liu Y M and Zhao Z Y 2003 *Appl. Phys. Lett.* **82** 4253
[12] Zhang X J, Ju W G, Gu M M, Meng X M, Shi W S, Zhang X H and Lee S T 2005 *Chem. Commun.* 4202
[13] Liang C, Terabe K, Tsuruoka T, Osada M, Hasegawa T and Aono M 2007 *Adv. Funct. Mater.* **17** 1466
[14] Liang C H, Terabe K, Hasegawa T, Aono M and Iyi N 2007 *J. Appl. Phys.* **102** 124308
[15] Lee W, Scholz R, Niesch K and Gösele U 2005 *Angew. Chem. Int. Edn* **44** 6050
[16] *CRC Handbook of Chemistry and Physics* 2007 (Boca Raton, FL: CRC Press)
[17] Lee J S, Adams S and Maier J 2000 *Solid State Ion.* **136** 1261
[18] Guo Y G, Lee J S and Maier J 2006 *Solid State Ion.* **177** 2467
[19] Brumlik C J and Martin C R 1991 *J. Am. Chem. Soc.* **113** 3174
[20] Davis B L and Johnson L R 1974 *Cryst. Lattice Defects* **5** 235
[21] Harvey G and Fletcher N H 1980 *J. Phys. C: Solid State Phys.* **13** 2969
[22] Vukic M R, Veselinovic D S and Markovic V G 2007 *J. Serb. Chem. Soc.* **72** 857